

Manufacturing and Industrial Processes sector: Iron & Steel Manufacturing Emissions



Verity Crane and George Ebri

Authors affiliated with TransitionZero and Climate TRACE

1. Introduction

Steel production is both energy and emissions intensive, representing about 8% of total energy demand and 7% of global energy sector carbon emissions (IEA, 2020). The emissions intensity of steel production is due to its reliance on coal. At the same time, steel is vitally important to the global economy, used in buildings, infrastructure, weapons, vehicles and furniture. Due to its importance to modern society, steel demand is expected to grow for the foreseeable future (IEA, 2020). Steel production is also relatively centralised, with China accounting for over half of global production, followed distantly by India (7.4%), Japan (4.6%) and the U.S. (4.3%) (WSA, 2024).

Steelmaking has two main metallic inputs: iron ore and recycled steel scrap. Around 70% of the total metallic input to steel production globally is derived from iron ore, with scrap making up the rest. Primary steel is produced using blast furnaces, with this route accounting for the majority of this sector's emissions. Secondary (or scrap-based) production is carried out in electric furnaces and is around one-eighth as energy-intensive as production from iron ore, using electricity – as opposed to coal – as the main energy input (IEA, 2020).

Steel production can be used as a proxy for emissions. By estimating facility-level production, we are therefore able to estimate changes in emissions and guide climate policy. As with any such globally traded commodity, steel production is characterised by fierce competition amongst producers. Consequently, facility-level data is rarely made publicly available. In most cases it is only possible to obtain steel production at the country level (WSA, 2024; NBSC, 2024) which is often released with substantial delays (~ 3 months). EU and U.S. plant-level emissions data can be sourced from respective registers (E-PRTR, 2024; US EPA, 2024), but this only accounts for around 10% of global production.

In this work we look to address both the temporal and spatial limitations in traditional reporting of steel production/emissions to provide more timely facility-level data. More specifically, we have aimed to deliver steel production and emissions estimates on a monthly basis for all sources identified on Global Energy Monitor's Global Iron and Steel Tracker (GIST) database (GEM, 2024). We have achieved this by primarily using satellite-derived hotspot data which can capture variation in activity for certain types of steel facilities.

2. Materials and Methods

This section provides a high-level overview of the datasets and associated pipelines used to derive emission estimates for a steel plant.

Direct emissions are released during the manufacturing of crude steel, with estimates varying by different production routes, namely blast furnace-basic oxygenation furnace (BF-BOF), direct reduced iron-electric arc furnace (DRI-EAF) and electric arc furnaces (EAF). A simplified overview of the steel production value chain from raw materials to final steel products is available in Appendix 1, section 7.1.

Given the lack of source-level emission data available publicly, a standardised “bottom-up” approach is used to quantify the emissions. This process is characterised by first estimating production levels at each plant, then subsequently applying a production-specific emissions factor to estimate emissions. Two approaches were used to estimate source level emissions as shown in Figure 1 below.

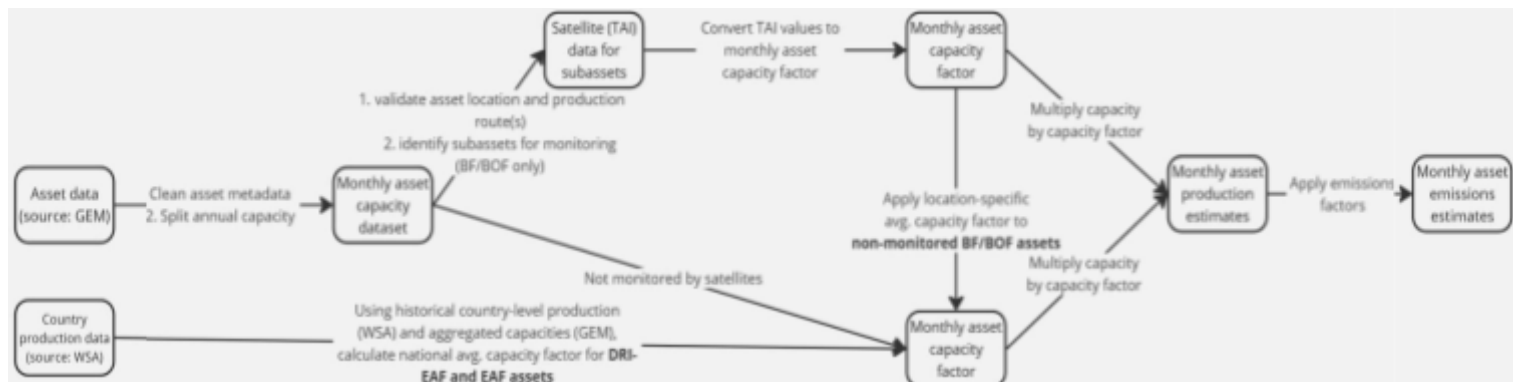


Figure 1 Flowchart of the methodology to calculate plant-level emissions for global steel assets.

2.1. Materials

2.1.1. Steel inventory dataset

GEM provides facility-level information such as location, owner, capacity, age, product type and technology type via the GSPT that includes every iron and steel plant currently operating with a capacity of more than 500 thousand tonnes. The GSPT also includes all plants meeting that capacity threshold that have been proposed or under construction since 2017 and retired or mothballed since 2020. In total there are 1,163 unique steel facilities with an annual production capacity of 3.4 billion tonnes across 89 countries. We manually validated the position of all the plants using geolocation data from Google Maps API (Google Maps, 2024) and OpenStreetMap (OpenStreetMap, 2024).

Figure 2 shows how steel mills are distributed globally with high concentration of sources in China. The map also highlights countries with little to no steel production, mainly concentrated in Sub-Saharan

Africa, Latin America and Southeast Asia.

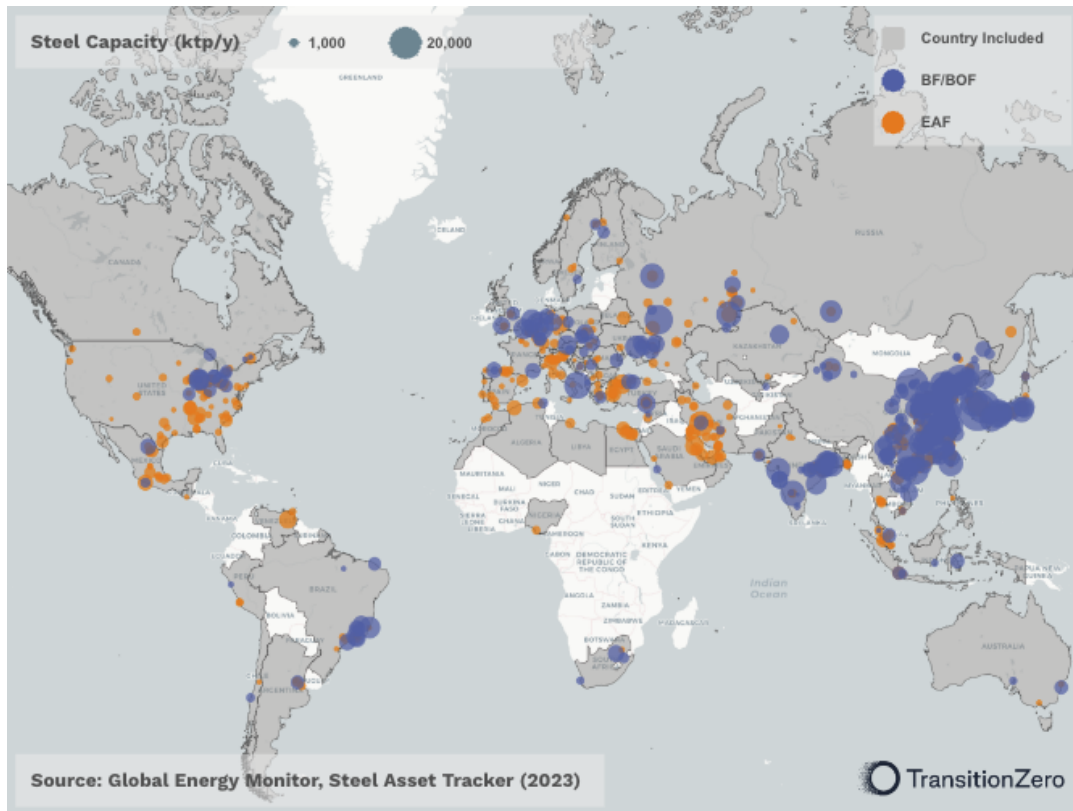


Figure 2 Global map showing operating steel plants as of 2023. Countries included in steel emissions monitoring are shaded in grey. EAF facilities (shown in orange) and BF-BOF facilities (shown in blue).

2.1.2. Remote sensing datasets

Satellite-derived production estimates make use of multispectral imagery from two different collections:

- The European Space Agency (ESA) Copernicus Sentinel mission with a resolution of 20 m and a combined 5-day equator revisit with two satellites:
 - Sentinel 2A: with imagery available since 2015 (ESA, 2024).
 - Sentinel 2B: with imagery available since 2017 (ESA, 2024).

Both Sentinel-2 satellites have a MultiSpectral Instrument (MSI) that can measure wavelengths from ~443 - ~2190 nm (blue to shortwave infrared (SWIR)) at 10-60 m spatial resolutions.

- The U.S. Geological Survey (USGS) and National Aeronautics and Space Administration (NASA) Landsat program with a resolution of 30 m and a combined 8-day revisit:
 - Landsat-8: with imagery available since 2013 (NASA and USGS, 2024a).
 - Landsat-9: with historical images available from 2021 (NASA and USGS, 2024b).

Both Landsat-8 and Landsat-9 have an Operational Land Imager (OLI) that can measure wavelengths from ~435 - ~1384 nm (blue to thermal infrared) at 15-100 m spatial resolutions.

All satellite datasets were sourced and processed using Google Earth Engine (Google Earth Engine, 2024a, 2024b, 2024c). From each satellite dataset, we relied on the surface reflectance products and computed the ratio of the difference between two SWIR bands and NIR bands of each satellite. This is based on the study to detect high-temperature anomalies from Sentinel-2 MSI images where a tri-spectral thermal anomaly index (TAI) that jointly uses the two high-temperature sensitive SWIR bands and the high-temperature-insensitive NIR band to enhance High Temperature Anomalies (Yongxue et al., 2021). For the respective satellite collections, we infer the TAI through the following equations:

- Sentinel-2A/B: $TAI = \frac{(B12 - B11)}{(B8a)}$
- Landsat-8/9: $TAI = \frac{(B7 - B6)}{(B5)}$

Where B# refers to the band number for the specific satellite. This ratio was used to identify thermal anomalies within the temperature range of industrial processes, while eliminating most of the noise from reflectance interference. Pixel values between the Sentinel 2A/B MSI and Landsat OLI were harmonised using NASA's band pass adjustments allowing the two image collections to be used as if they were a single collection (NASA, 2018). The harmonised dataset ensured higher revisit for time-series surface applications. Partial images (coverage of the steel facility's boundaries less than 80%) and cloudy images (more than 20% clouds) were excluded. Figure 3 shows an example of TAI with identified hotspots at a steel plant.

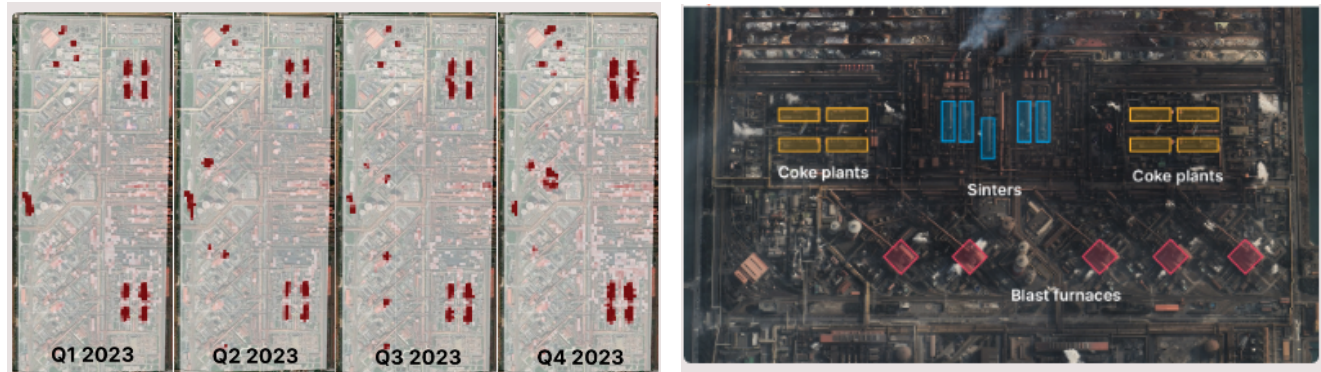


Figure 3 Left: Identified hotspots at POSCO's Gwangyang steel plant, South Korea, during different quarters in 2023. Right: Identified sub-assets within the facility based on thermal anomalies. Sources: modified Copernicus and USGS data, ESRI base map.

2.1.3. Production datasets

Aggregated national steel production used in our models is primarily sourced from WSA on a monthly basis.

2.1.4. Emissions factors dataset

The direct emissions factor and electricity use were sourced from Mission Possible Partnership's (MPP, 2024) Steel Transition Strategy, which provides a global average number for different steel production routes.

2.1.5. Percentage of scrap used in EAF

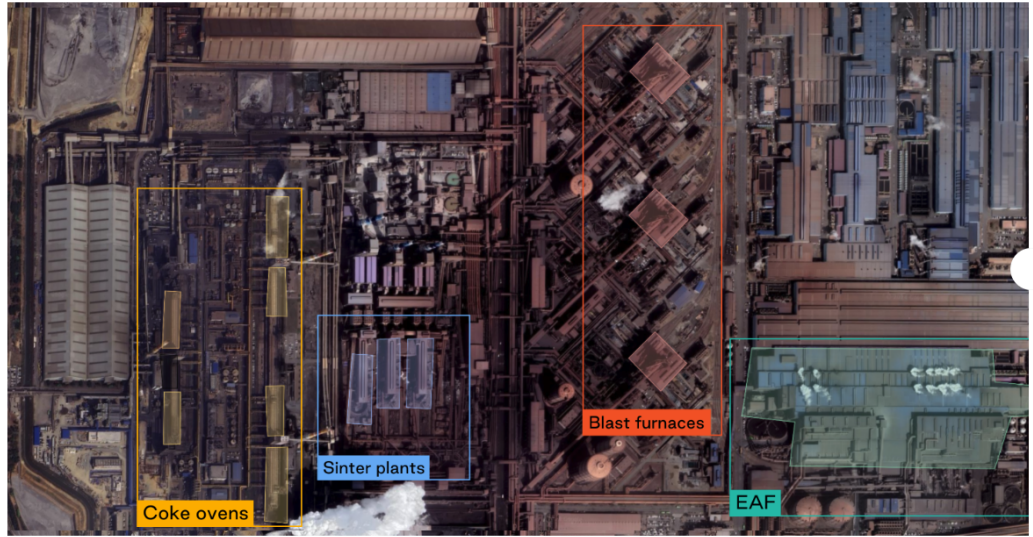
The composition of the feedstock mix used in EAF production was provided by GEM, including the percentages of scrap, DRI and sponge iron, and pig iron. This data was used to adjust the emission factor for EAF production route.

2.2. Methods

2.2.1. Production methodology

Two approaches were used to estimate source level production. As a priority, satellite-derived production estimates were used whenever a facility released enough heat to be captured by a satellite's sensor that can measure short-wave infrared (SWIR) and near infrared (NIR) wavelengths (Zhou *et al.*, 2018; Marchese *et al.*, 2019; Liangrocrapart, Khetkeeree and Petchthaweetham, 2020). This is the case for BF-BOF facilities which have several units that function at temperatures higher than 1,200°C. These hotspots include signals from BFs, coke ovens, sinter plants, pellet plants and BOFs.

Our methodology scours satellite imagery for heat signatures from the operating steel plants. Each steel production unit, once identified, is outlined with a hand-drawn polygon, as shown in Figure 4. Using GSPT as a foundation, we built a global dataset of blast furnaces, coke oven batteries, sinters and pellet plants with the help of our satellite-based hotspot methodology. The current dataset spans 40 countries and contains the location, shape, crude steel capacity and operation start year for 345 steel plants, and the location, shape, and type for 2,301 of their associated sub-assets. More details on the methodology and dataset are available on the TransitionZero website (<https://www.transitionzero.org/insights/steel-data-explainer>).



Source: [Google Earth Engine timelapse, IZ Steel Asset Polygons Dataset](#)

TransitionZero

Figure 4 Zooming in on Hyundai Steel Integrated Steel Works (Dangjin, South Korea), with identified sub-asset polygons.

The intensity of the hotspot above each identified unit is calibrated against the monthly country level data source from WSA (2024) to estimate plant activity in each month.

For BF-BOF facilities that were not monitored by satellites, we extrapolated the regional or global average of satellite derived utilisation rates if we monitored other BF-BOF facilities in the same country or not. For all the other plants where hotspots cannot be measured (EAFs for instance), we applied a regional average utilisation rate based on historical national production and aggregated capacity.

2.2.2. Emissions methodology

Facility level direct and indirect emissions were derived by multiplying the production estimates with the relevant emissions factors. In the case of EAF production, the proportion of scrap in the feedstock mix was used to refine the estimation of emission factors. To calculate the effective emission factor Ea(EAF) based on the actual feedstock composition, the following weighted average formula was applied:

$$E_a(EAF) = E_a^{scrap} \times pc_{scrap} + E_a^{DRI} \times pc_{DRI} + E_a^{pig\ iron} \times pc_{pig_iron}$$

Where:

E_a^{scrap} , E_a^{DRI} , and $E_a^{pig\ iron}$ represent the emission factors for EAF production using 100% scrap, DRI, and pig iron, respectively.

pc_{scrap} , pc_{DRI} , and pc_{pig_iron} are the corresponding proportions of each feedstock type used.

To determine the proportion of each feedstock used at a given asset, a weighted average was calculated based on the capacities of its EAF units.

The indirect emissions factors were calculated using the average electricity use for different production routes (MPP contributors, 2024) and the regional grid intensity (Ember contributors, 2024). For plants with multiple steel production routes, the emissions factor was calculated based on the weighted share of production capacity.

2.3. Coverage

Based on 2023 data, asset level emissions estimates accounted for 81% (2.7 Gt-CO₂) of the sectors' direct emissions. While satellite-monitored steel facilities represent around 40% of total sources, these plants contributed to about three-quarters of the total asset level emissions.

3. Results and analysis

Figure 5 illustrates the relationship between satellite-derived Thermal Anomaly Index (TAI) and the corresponding emissions for a steel plant in France. The data demonstrates that, for most months, estimated emissions (based on production levels) align closely with fluctuations in TAI. For example, both peak just after July 2021, followed by a decrease after January 2022.

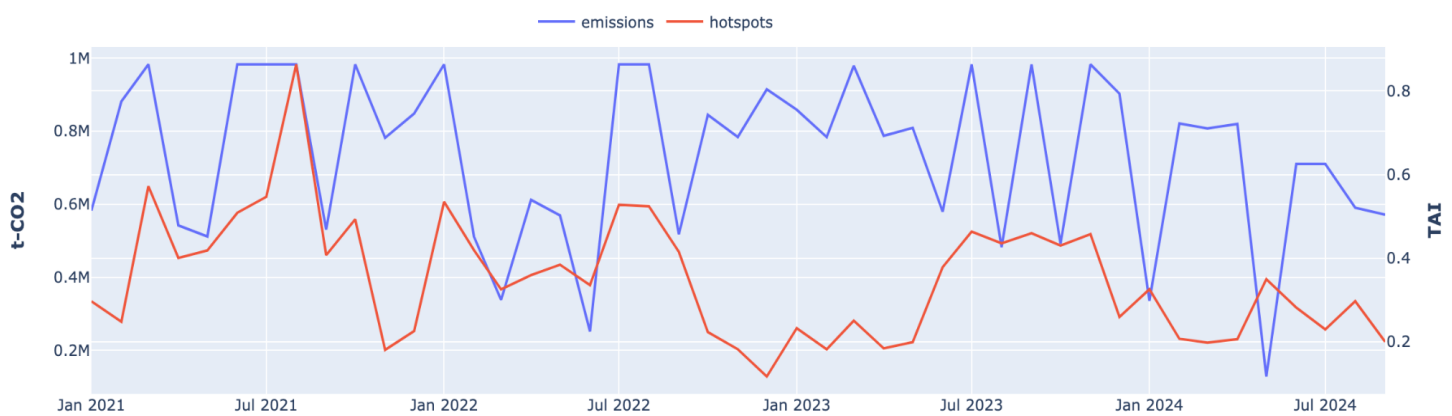


Figure 5 Satellite-based Thermal Anomaly Index (TAI; red solid line) and estimated emissions (blue solid line) at ArcelorMittal's Fos-sur-Mer steel plant during Jan'21- Sep'2024.

However, further calibration is needed to enhance the model that translates TAI into asset-level production, as TAI data can vary significantly by asset depending on factors like equipment type, age, geographic location, and other operational conditions. The TAI values presented here are derived from the hotspot data shown in Figure 6.



Figure 6 Satellite-detected hotspots (upper centre and centre right) over ArcelorMittal's Fos-sur-Mer steel plant during Sep. 2024.

Table 1 and 2 shows the biggest producers and emitters in the steel industry at country and plant level, respectively. China accounts for more than half of the global steel production and emissions, and has some of the largest and most emitting steel plants (Table 2).

Table 1 Top 10 emitters in the steel sector in 2023 - by country (direct emissions only)

country	CO ₂ emissions (MtCO ₂)
China	2,241
India	162
Japan	160
Russia	125
S Korea	117
USA	72
Germany	64
Brazil	61
Vietnam	32
Turkey	27

Table 2 Top 10 emitting steel plants in 2023 (direct emissions only)

plant name	country	plant capacity (Mt)	CO ₂ emissions (MtCO ₂)
POSCO Gwangyang steel plant	S Korea	23	41.6
Angang Steel Co Ltd.	China	24.1	38.9
Baoshan Iron and Steel Co Ltd.	China	18.6	34
Wuhan Iron and Steel Co., Ltd.	China	15.9	31.3
Rizhao Steel Holding Group Co Ltd	China	13	27.9
POSCO Pohang steel plant	S Korea	17.4	27.4
Zhangjiagang Hongchang Steel Co Ltd.	Japan	17.6	27.3
Shougang Jingtang United Iron & Steel Co Ltd	China	13.7	26.9
JFE West Japan Works (Fukuyama) steel plant	Japan	13	26.2
Baosteel Zhanjiang Iron & Steel Co Ltd.	Japan	12.5	26

4. Conclusions and Discussions

In this work a new approach has been implemented to estimate steel production and emissions at facility level on a monthly basis for 866 operating steel plants in 89 countries in the GEM contributors (2024) database.

Our modelling approach consists of estimating facility level production and then applying the relevant emissions factors to yield emissions estimates. The approach for estimating production was dependent upon the facility type. The activity of BF-BOF facilities were tracked by satellite-based thermal anomalies as these plants contain several units - BFs, coke plants, sinter plants, BOFs - that operate at temperatures in excess of 1,200°C. Such high temperatures present a strong signal which can be used as a proxy for inferring activity at a given time. The production for other facilities that do not have such high temperature units, such as DRI-EAF and EAF facilities, were instead estimated via a regional utilisation rate based on historical production and capacity data. The satellite-based approach was advantageous in that it can provide dynamic estimates of plant activity. Limitations in this approach may arise from either the incorrect detection of relevant hotspots or lack of enough data due to cloud cover. In both cases a larger study period is expected to improve the accuracy of our model estimates.

Ultimately, this work has shown that timely facility level production and emissions can be obtained without the need to rely upon factory published figures, often years out of date, and may open pathways to assist in future climate policy. Future works may benefit from greater availability of asset data for training a model.

5. Supplementary metadata section

Steel sector CO₂ emissions have been reported for individual sources from January 2021. The emissions described here represent a subset of specific country-level emissions estimates from the Climate TRACE manufacturing sector. All data is freely available on the Climate TRACE website (<https://climatetrace.org/>). A detailed description of what is available is described in Tables 3 - 5.

Table 3 Details on the asset metadata

General Description	Definition
Sector definition	<i>Emissions from iron and steel production</i>
UNFCCC sector equivalent	<i>2.C.1 Iron and steel production</i>
Temporal Coverage	<i>2021 - present</i>
Temporal Resolution	<i>Monthly</i>
Data format	<i>CSV</i>
Coordinate Reference System	<i>None. ISO3 country code provided</i>
Number of sources available for download	<i>866 sources covering 89 countries</i>
What emission factors were used?	<i>Global average emission factors for different production routes</i>
What is the difference between a “0” versus “NULL/none/nan” data field?	<i>“0” values are for true non-existent emissions. If we know that the sector has emissions for that specific gas, but the gas was not modelled, this is represented by “NULL/none/nan”</i>
total_CO2e_100yrGWP and total_CO2e_20yrGWP conversions	<i>Climate TRACE uses IPCC AR6 CO₂e GWPs. CO₂e conversion guidelines are here: https://www.ipcc.ch/report/ar6/wg1/downloads/report/IPCC_AR6_WGI_FullReport_small.pdf</i>

Table 4 Definition of the fields in asset dataset

Data attribute	Definition
sector	manufacturing
source_sub-sector_name	iron and steel
source_definition	emissions from iron and steel production
start_date	start date for time period of emissions estimation (YYYY-MM-DD format)
end_date	end date for time period of emissions estimation (YYYY-MM-DD format)
asset_identifier	internal identifier

Data attribute	Definition
asset_name	name of the facility
iso3_country	ISO 3166-1 alpha-3 country code
location	well-known text (WKT) point location
type	manufacturing method
capacity	monthly plant capacity
capacity_factor	utilisation rate of steel mills
activity	production estimates
CO2_emissions_factor	direct emissions factor (t-CO2/t-steel)
CH4_emissions_factor	not used; N/A
N2O_emissions_factor	not used; N/A
CO2_emissions	direct emissions estimates (t-CO ₂)
CH4_emissions	not used; N/A
N2O_emissions	not used; N/A
total_CO2e_100yrGWP	100 years global warming potential (t-CO ₂ e)
total_CO2e_20yrGWP	20 years global warming potential (t-CO ₂ e)
other1	direct and indirect emissions factor: includes electricity use
other2	direct and indirect emissions: includes electricity use
other3	electricity use factor (MWh/t-steel)
other4	electricity consumption (MWh)
other5	grid emissions intensity (t-CO ₂ /MWh)
other6	model methodology (e.g. satellite_monitored or extrapolation)
other7	grid marginal operating emissions intensity (t-CO ₂ /MWh)
other9	Percentage of scrap utilized in EAF
model_number	version of the model (e.g. 1, 2, ...)

Table 5 Definition for confidence and uncertainty in emissions.

Data attribute	Confidence Definition	Uncertainty Definition
type	<ul style="list-style-type: none"> <i>Very low:</i> Based on highly speculative or obsolete information. Very low level of confidence in the accuracy of steel plant classification. <i>Low:</i> Limited or somewhat outdated data. Low level of confidence in the classification's correctness. <i>Medium:</i> A mix of historical and more recent data. A medium level of confidence in its accuracy. <i>High:</i> Grounded in comprehensive and recent data. A high level of confidence in the precise classification of the steel plant. <i>Very high:</i> Extensive, up-to-date, and verified data. A very high level of confidence in the accurate and detailed identification of the steel plant. 	Not used; N/A
capacity	<ul style="list-style-type: none"> <i>Very low:</i> Limited or outdated data, and significant uncertainties exist. <i>Low:</i> Outdated and/or incomplete data. <i>Medium:</i> A mix of historical and recent data. <i>High:</i> Comprehensive and recent data updates. High level of certainty. <i>Very high:</i> Extensive, up-to-date, and verified data. A very high level of certainty. 	Not used; N/A
capacity_factor	<ul style="list-style-type: none"> <i>Very low:</i> Data is sparse or highly unreliable. Considerable uncertainty in capacity factor estimations. <i>Low:</i> Moderate uncertainty in capacity factor calculations. <i>Medium:</i> Data is sufficiently available, though not comprehensive. No absolute accuracy in capacity factor estimations. <i>High:</i> High confidence in the accuracy of capacity factor calculations. <i>Very high:</i> Derived from thorough and validated data sources. Very high precision of capacity factor estimations. 	Not used; N/A
activity	<ul style="list-style-type: none"> <i>Very low:</i> Largely speculative or based on outdated information. A very low level of confidence in activity assessments. <i>Low:</i> Limited or somewhat outdated sources. A low level of confidence in the activity assessments. <i>Medium:</i> A mix of historical and more recent data. Medium level of confidence in activity insights. <i>High:</i> Detailed and current operational data ensures a high level of confidence in the accuracy of activity assessments. <i>Very high:</i> Extensive, verified, and up-to-date data. A very high level of confidence in their accuracy. 	±10% of production estimates (based on IPCC)

Data attribute	Confidence Definition	Uncertainty Definition
CO2_emissions_factor	<ul style="list-style-type: none"> <i>Very low:</i> Highly uncertain due to insufficient or unreliable data. <i>Low:</i> Estimated from incomplete data. Low confidence level in its precision. <i>Medium:</i> A mix of historical and more recent data. Medium level of confidence in their accuracy. <i>High:</i> Derived from comprehensive and recent data. A high level of confidence in their precision. <i>Very high:</i> Based on extensive and validated data, providing a very high level of confidence in their precision. 	±10% of assumption (based on IPCC)
CH4_emissions_factor	Not used; N/A	Not used; N/A
N2O_emissions_factor	Not used; N/A	Not used; N/A
CO2_emissions	<ul style="list-style-type: none"> <i>Very low:</i> Based on very rough estimations or outdated information. A very low level of confidence in its accuracy. <i>Low:</i> Estimated from incomplete data. Low confidence level in its precision. <i>Medium:</i> A mix of historical and more recent data. Medium level of confidence in their accuracy. <i>High:</i> Derived from comprehensive and recent data. A high level of confidence in their precision. <i>Very high:</i> Based on extensive and validated data, providing a very high level of confidence in their precision. 	±20% of emissions estimates
CH4_emissions	Not used; N/A	Not used; N/A
N2O_emissions	Not used; N/A	Not used; N/A
total_CO2e_100yrGWP	<ul style="list-style-type: none"> <i>Very low:</i> Based on very rough estimations or outdated information. A very low level of confidence in its accuracy. <i>Low:</i> Estimated from incomplete data. Low confidence level in its precision. <i>Medium:</i> A mix of historical and more recent data. Medium level of confidence in their accuracy. <i>High:</i> Derived from comprehensive and recent data. A high level of confidence in their precision. <i>Very high:</i> Based on extensive and validated data, providing a very high level of confidence in their precision. 	±20% of emissions estimates
total_CO2e_20yrGWP	<ul style="list-style-type: none"> <i>Very low:</i> Based on very rough estimations or outdated information. A very low level of confidence in its accuracy. 	±20% of emissions estimates

Data attribute	Confidence Definition	Uncertainty Definition
	<ul style="list-style-type: none"> • <i>Low</i>: Estimated from incomplete data. Low confidence level in its precision. • <i>Medium</i>: A mix of historical and more recent data. Medium level of confidence in their accuracy. • <i>High</i>: Derived from comprehensive and recent data. A high level of confidence in their precision. • <i>Very high</i>: Based on extensive and validated data, providing a very high level of confidence in their precision. 	

Permissions and Use: All Climate TRACE data is freely available under the Creative Commons Attribution 4.0 International Public License, unless otherwise noted below.

Citation format: Crane, V., Ebri, G. (2025). *Manufacturing and Industrial Processes sector - Iron & Steel Manufacturing Emissions*. TransitionZero, UK, Climate TRACE Emissions Inventory - <https://climatetrace.org>

The above usage is not warranted to be error free and does not imply the expression of any opinion whatsoever on the part of Climate TRACE Coalition and its partners concerning the legal status of any country, area or territory or of its authorities, or concerning the delimitation of its borders.

Disclaimer: The emissions provided for this sector are our current best estimates of emissions, and we are committed to continually increasing the accuracy of the models on all levels. Please review our terms of use and the sector-specific methodology documentation before using the data. If you identify an error or would like to participate in our data validation process, please [contact us](#).

6. References

1. Ember (2024) ‘*Regional grid intensity retrieved from: Monthly Electricity Data*’, Ember. Available at: <https://ember-energy.org/data/monthly-electricity-data/>
2. E-PRTR (2024) ‘*Steel emissions data retrieved from: E-PRTR*’, European Pollutant Release and Transfer Register. Available at: <http://prtr.ec.europa.eu/>
3. ESA (2024) ‘*Satellite images data retrieved from: Copernicus Sentinel-2 ESA*’, European Space Agency. Available at: https://www.esa.int/Applications/Observing_the_Earth/Copernicus/Sentinel-2
4. GEM (2024) ‘*Steel inventory data retrieved from: Global Steel Plant Tracker*’, Global Energy Monitor. Available at: <https://globalenergymonitor.org/projects/global-steel-plant-tracker/>
5. Google Earth Engine (2024a) *Landsat 8 Datasets in Earth Engine*, Google Developers. Available at: <https://developers.google.com/earth-engine/datasets/catalog/landsat-8>
6. Google Earth Engine (2024b) *Landsat 9 Datasets in Earth Engine*, Google Developers. Available at: <https://developers.google.com/earth-engine/datasets/catalog/landsat-9>
7. Google Earth Engine (2024c) *Sentinel-2 Datasets in Earth Engine*, Google Developers. Available at: <https://developers.google.com/earth-engine/datasets/catalog/sentinel-2>

8. Google Maps contributors (2024) ‘Steel inventory data retrieved from: Google Maps’. Google. Available at: <https://www.google.co.uk/maps>
9. IEA (2020) ‘Iron and Steel Technology Roadmap - Towards more sustainable steelmaking’. International Energy Agency, p. 190.
10. Kato, S. (2021) *Automated classification of heat sources detected using SWIR remote sensing Elsevier Enhanced Reader*. Available at: <https://doi.org/10.1016/j.jag.2021.102491>
11. Liangrocapart, S., Khetkeeree, S. and Petchthaweetham, B. (2020) ‘Thermal Anomaly Level Algorithm for Active Fire Mapping by Means of Sentinel-2 Data’, in 2020 17th International Conference on Electrical Engineering/Electronics, Computer, Telecommunications and Information Technology (ECTI-CON).
12. Marchese, F. et al. (2019) ‘A Multi-Channel Algorithm for Mapping Volcanic Thermal Anomalies by Means of Sentinel-2 MSI and Landsat-8 OLI Data’, *Remote Sensing*, 11(23), p. 2876. Available at: <https://doi.org/10.3390/rs11232876>
13. MPP (2024), ‘Steel emissions factor retrieved from: MPP’, Mission Possible Partnership Steel Transition Strategy. Available at: <https://www.missionpossiblepartnership.org/action-sectors/steel/>
14. NASA (2018) ‘Band Pass Adjustment’, National Aeronautics and Space Administration. Available at: <https://hls.gsfc.nasa.gov/algorithms/bandpass-adjustment/> (Accessed: 1 June 2024).
15. NASA and USGS (2024a) ‘Satellite images data retrieved from: Landsat-8 NASA/USGS’, National Aeronautics and Space Administration and United States Geological Survey. Available at: <https://www.usgs.gov/landsat-missions/landsat-8>
16. NASA and USGS (2024b) ‘Satellite images data retrieved from: Landsat-9 NASA/USGS’, National Aeronautics and Space Administration and United States Geological Survey. Available at: <https://www.usgs.gov/landsat-missions/landsat-9>
17. NBSC (2024) ‘Chinese steel production data retrieved from: NBSC’, National Bureau of Statistics of China. Available at: <http://www.stats.gov.cn/english/>
18. OpenStreetMap (2024) ‘Steel inventory data retrieved from: OpenStreetMap’. OpenStreetMap. Available at: <https://www.openstreetmap.org/>
19. US EPA (2024) ‘Steel emissions data retrieved from: US EPA’, United States Environmental Protection Agency. Available at: <https://www.epa.gov/>
20. WSA (2024) ‘Steel production data retrieved from: Worldsteel’, Worldsteel Association. Available at: <https://worldsteel.org/wp-content/uploads/World-Steel-in-Figures-2024.pdf>
21. Yongxue, L., Weifeng, Z., Bihua, X., Wenxuan, X., Wei, W. (2021) ‘Detecting high-temperature anomalies from Sentinel-2 MSI images’, *ISPRS Journal of Photogrammetry and Remote Sensing*, 177, p. 174-193, Available at: <https://doi.org/10.1016/j.isprsjprs.2021.05.00>
22. Zhou, Y. et al. (2018) ‘A Method for Monitoring Iron and Steel Factory Economic Activity Based on Satellites’, *Sustainability*, 10(6), p. 1935. Available at: <https://doi.org/10.3390/su10061935>

7. Appendices

7.1. Appendix 1: Overview of the steel production process

The principal inputs to steelmaking today are iron ore, energy, limestone and scrap. Iron ore and scrap are used to provide the metallic charge, with scrap having a much higher metallic concentration than iron ore. Energy inputs provide heat to melt the metallic input, and in the case of iron ore, to chemically remove oxygen. Limestone is used at various stages of the steelmaking process to help remove impurities. Figure 7 highlights these main routes to produce steel.

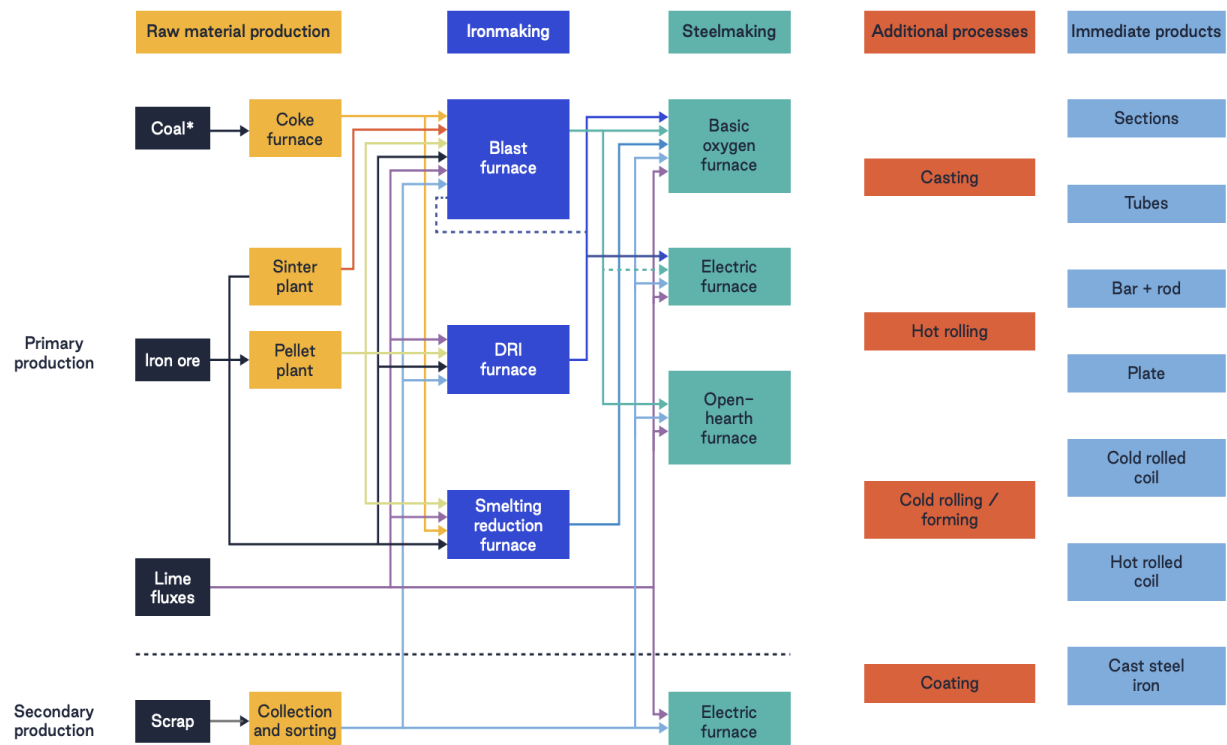


Figure 7 Steel production routes - adapted from IEA (2020).